

Determination of Proportionality Constants from Experiments to Develop a Force Model for Reaming Process.

C. Raghavendra Kamath, M.S., M.Tech.^{1*} and K.K. Appu Kuttan, Ph.D.²

¹Research Scholar, Department of Mechanical Engineering, Manipal Institute of Technology, Manipal, Karnataka, India

²Professor, Department of Mechanical Engineering, National Institute of Technology, Surathkal, Karnataka, India.

*E-mail: mitian99@rediffmail.com

ABSTRACT

Mechanistic models assume that cutting forces acting on reamer flutes, especially the tangential forces, are proportional to chip cross sectional area. The constant of proportionality relating the cutting force and chip area are obtained through experimentation. Drilling process was used to formulate the proportionality constant in terms of specific cutting energy coefficients. In this paper, an attempt has been made to determine specific cutting energy coefficients using drilling operation for different materials and obtaining proportionality constants for machining. The paper also includes static force modeling for reaming operation and graphical presentation of the results.

(Keywords: mechanistic, reamer, static force, tangential force, specific cutting coefficients)

INTRODUCTION

Metal cutting is one of the basic operations in manufacturing industries used to produce the parts of desired dimensions and shape. Metal cutting constitutes a complex process involving the diversity of physical phenomenon such as large plastic deformation, frictional contact, thermo-chemical coupling, and chip and burr formation mechanisms. A great deal of research [1-5] and [14-16] has been devoted to understanding the mechanism of machining with the objective of obtaining more effective tool and manufacturing operations.

Over the last several years, a considerable amount of research has been carried out to develop mechanistic force model for variety of

machining processes, including end milling, face milling, boring, turning and broaching. These models have been employed in a number of designs, operations planning and process control setting to predict both the cutting forces and the resulting machined surface error.

In the literature [6-9], two different approaches have been adopted for the prediction of the cutting force system. The first method is based on the work done by Merchant, and involves a study of the cutting mechanics and the prediction of the shear angle in metal cutting. Both analytical and empirical models for shear angle prediction have been attempted. Lee and Shaffer [1951] applied slip line theory to machining to develop the equation for predicting the shear angle.

Usui, et al. [1978] developed a model that was based on the minimum energy criterion for predicting the chip flow angle and empirical models were used for predicting both the friction angle and the shear angle. This approach generally requires experimentation of a more fundamental cutting mechanics nature to achieve the measurement and prediction of the shear angle.

In this paper, an attempt has been made to determine specific energy coefficients experimentally for various materials such as aluminum, cast iron, and mild steel. Drilling process was used for the calibration purpose for determining cutting forces through mechanistic modeling during reaming operation. Mechanistic model has been developed to compute static forces. The results are presented graphically.

COMPUTATION OF SPECIFIC ENERGY CONSTANTS FOR PREDICTING THE CUTTING FORCES

Mechanistic Modeling Approach: In the mechanistic modeling approach, for any machining process the basic equations that relates the F_n , F_t and F_a to the chip cross sectional area are given by:

$$\begin{aligned} F_t &= K_t A_c \\ F_n &= K_n A_c \\ F_a &= K_a A_c \end{aligned} \quad (1)$$

where F_n , F_t and F_a are the three dimensional forces acting on the tool tip. The specific cutting energy coefficients depend on t_c , v_c and γ_a of the cutting tool. Mathematically,

$$\begin{aligned} K_t &= e^{a_0 + a_1 \log t_c + a_2 \log v_c + a_3 \log t_c \log v_c + a_4 \log \gamma_a} \\ K_n &= e^{b_0 + b_1 \log t_c + b_2 \log v_c + b_3 \log t_c \log v_c + b_4 \log \gamma_a} \\ K_a &= e^{c_0 + c_1 \log t_c + c_2 \log v_c + c_3 \log t_c \log v_c + c_4 \log \gamma_a} \end{aligned} \quad (2)$$

The coefficients a_i 's, b_i 's and c_i 's ($i = 1, 2, 3, 4$) depend upon the tool and work piece material and range of cutting speed and chip thickness and they are independent of the machining process. Usually these coefficients are determined from calibration test for a given tool and work piece combination and given range of cutting conditions. Keeping the rake angle and the velocity of the tool movement as constant corresponding to reamer tool configuration, the equation (2) reduces to:

$$\begin{aligned} K_t &= e^{a_0 + a_1 \log t_c} \\ K_n &= e^{b_0 + b_1 \log t_c} \\ K_a &= e^{c_0 + c_1 \log t_c} \end{aligned} \quad (3)$$

The values of specific cutting energy coefficients can be determined using a simple calibration experiment. The experiments were conducted for drilling operation and specific cutting energy coefficients are determined.

Experimental Investigation: Several sets of drilling operation experiments were conducted in order to determine the specific cutting energy coefficients. Three experiments were conducted on each set of process. The first set of experiment was used to ascertain which tool and cutter geometry's variables affect the proportionality constants. The second set of experiments was used to develop adequate model for proportionality constant based on the important tool and cutter geometry variables, determined from first set of experiments. Experiments are repeated for aluminum, cast iron and mild steel for different depth of cut. Chip thickness area for the calibration purpose is measured from the chip curl. The volume of the chip is measured using water displacement method. After that, the chip curl is heated and elongated. The width of the chip, 'b' and length 'l' are measured using micrometer and Vernier caliper, respectively. Then, the actual chip thickness ' t_c ' is obtained by volume divided by the product of length and width, that is:

$$t_c = \frac{v}{b * l} \quad (4)$$

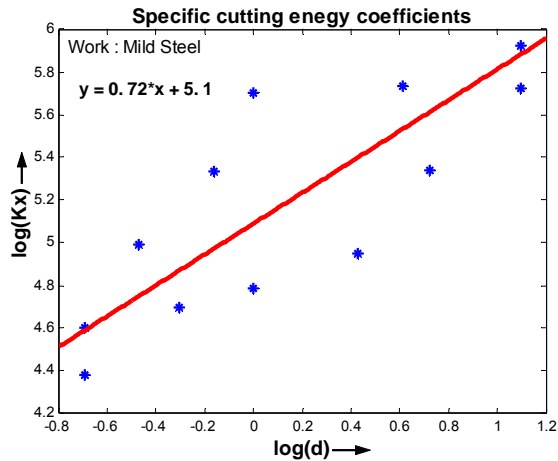
where 'v' is the volume of chip curl. Knowing the chip thickness and width of the cut, the chip load area can be computed as the product of actual chip thickness and width of the chip.

Results and Discussions: Figure 1 illustrates the cutting force versus chip thickness during drilling operation for the mild steel material. A linear curve fitting is made using MATLAB® software to determine the specific energy coefficients. Tool geometries were considered same as the reaming tool. Hence, the variation in specific cutting energy coefficients is not considered for the rake angle variation in the tool.

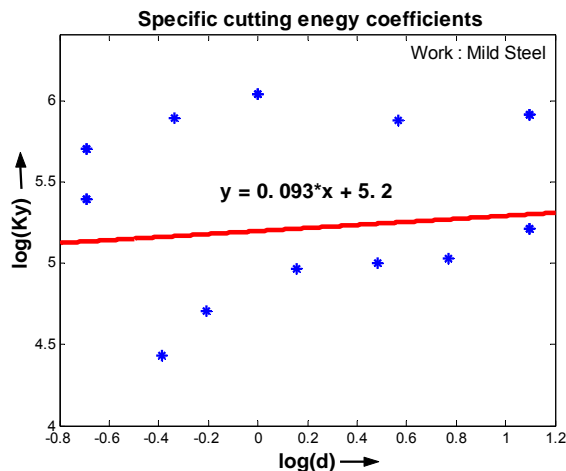
Table 1 gives the specific cutting energy coefficients for other materials like cast iron and aluminum obtained using the same method.

STATIC MODEL

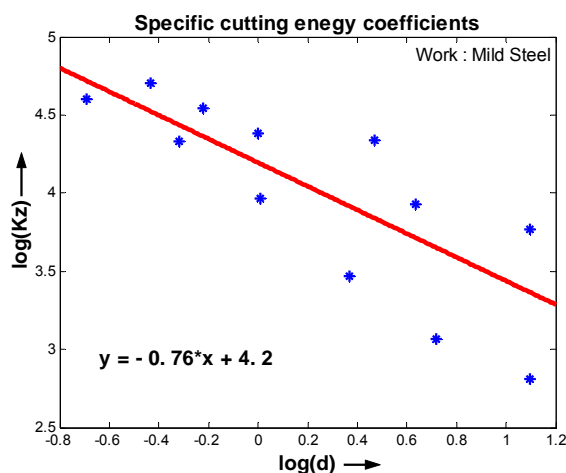
A static analysis calculates the effects of steady loading conditions on a structure, while ignoring inertia and damping effects, such as those caused by time-varying loads.



a) Graph for Determining a_0 and a_1



b) Graph for Determining b_0 and b_1



c) Graph for determining c_0 and c_1

Figure 1: Specific Cutting Energy Coefficients for Mild Steel During Drilling Operations.

Table 1: Specific Cutting Energy Coefficients During Drilling.

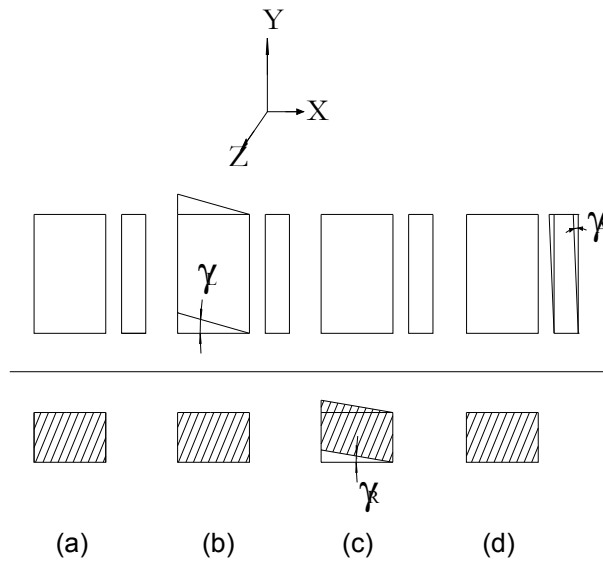
Material	a_0	a_1	b_0	b_1	c_0	c_1
Aluminum	5.5	0.51	4.9	1.4	2.7	-0.18
Mild steel	5.1	0.72	5.2	0.093	4.2	-0.76
Cast iron	4.8	0.39	5.7	-0.37	5.7	-0.37

A static analysis can, however, include steady inertia loads (such as gravity and rotational velocity), and time-varying loads that can be approximated as static equivalent loads. Static analysis is used to determine the displacements, stresses, strains, and forces in structures or components caused by loads that do not induce significant inertia and damping effects. Steady loading and response conditions are assumed, that is, the loads and the structure's response are assumed to vary slowly with respect to time. The most commonly used loads in static analysis include externally applied forces and pressures, steady-state inertial forces and temperature loads.

Early efforts in reaming analyzed it, considered as an orthogonal cutting process with the assumption that material is removed by one triangular tooth [3]. However, this assumption is not valid for the reamer. Hence, the model has been modified to predict the cutting forces during reaming operation by mechanistic model which consider the misalignment, ovality, and eccentricity. Figures 2 and 3 illustrate the three planar rotation of the cutting edge of an oblique cutting tool and the corresponding angles γ_A , γ_L and γ_R for the cutting edge of the reamer.

Chip Thickness Computation: The cutting reamer generates internal finish as successive cutting edges on the chamfered section of the reamer are rotated relative to the work while being fed at a rate per revolution equal to the lead.

Material is removed progressively from the wall of the hole until the final form is obtained. Although, cross sectional area of the material removed by the cutting edge of each chamfered flute is asymmetrical, the composite effect is truncated symmetrically.



a) Normal position. b) Rotated about z axis. c) Rotated about y axis d) Rotated about x-axis

Figure 2: Three Planar Angles of the Tool Cutting Edge.

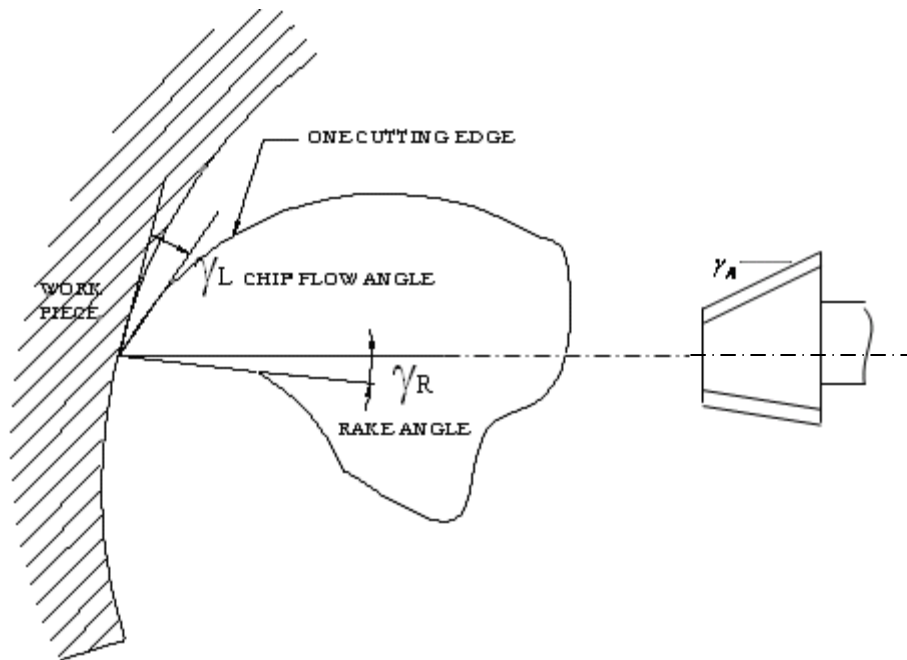


Figure 3: Reamer Rake Angle, Chip Flow Angle, and Lead Angle.

The chip load is computed as the un-deformed interference area of the tool and the work piece as a function of time. Also, the hole obtained after drilling is never perfect [11]. Therefore, the variation of the hole radius is to be taken into

consideration to compute the chip load. The chip load initially increases as the reamer penetrates into the work piece. It reaches a steady state when the tapered part of the reamer has fully engaged with the work piece. The increase in the

chip load in the entry phase of the reamer is given by the difference in successive trapezoidal areas T_i and T_{i-1} .

Figure 4 shows the chip load on the tooth in a helix plane parallel to the axis of the reamer. From the geometry of the reamer, and the hole radius, the points P_1, P_2, P_3, P_4 in the local X-Z coordinate frame can be found by interposing the interference area between the work piece and the reamer which is to be considered depends on the feed rate.

Similarly each trapezoidal section is interposed on the next trapezoidal section to form 2-D trapezoidal shaped regions. The trapezoidal section centroid is obtained. The trapezoidal section centroid is obtained as the intersection point of the lines joining the diagonals for the trapezoidal regions and as the intersection point obtained by joining lines from each point to the mid point of the opposite ends for the triangular region. Therefore, the instantaneous chip load area (area of the trapezoid) $dA_c(t)$ for engagement at any time t_i can be computed as:

$$dA_c(t) = 1/2 \left(\begin{vmatrix} 1 & 1 & 1 \\ x_1 & x_2 & x_3 \\ z_1 & z_2 & z_3 \end{vmatrix} + \begin{vmatrix} 1 & 1 & 1 \\ x_1 & x_3 & x_4 \\ z_1 & z_3 & z_4 \end{vmatrix} \right) \quad (5)$$

Average chip thickness, ' t_c ' can be computed as the ratio of the chip load area, $dA_c(t)$, to the cutting length, $l_c(t)$:

$$t_c(t) = \frac{dA_c(t)}{l_c(t)} \quad (6)$$

The moment arm i.e., radial distance of the centroid of the interference area of trapezoidal from the reamer axis, $c(t)$ is computed from the expression:

$$c(t) = \frac{1}{6[dA_c(i)]} \left(\begin{vmatrix} 1 & 1 & 1 \\ x_1 & x_2 & x_3 \\ z_1 & z_2 & z_3 \end{vmatrix} (x_1 + x_2 + x_3) + \begin{vmatrix} 1 & 1 & 1 \\ x_1 & x_3 & x_4 \\ z_1 & z_3 & z_4 \end{vmatrix} (x_1 + x_3 + x_4) \right) \quad (7)$$

Torque, Radial, and Thrust Force Computation: Once the normal and the frictional forces are known, they can be resolved into tangential direction, radial direction and along the axis of the reamer to obtain the torque, radial and thrust forces.

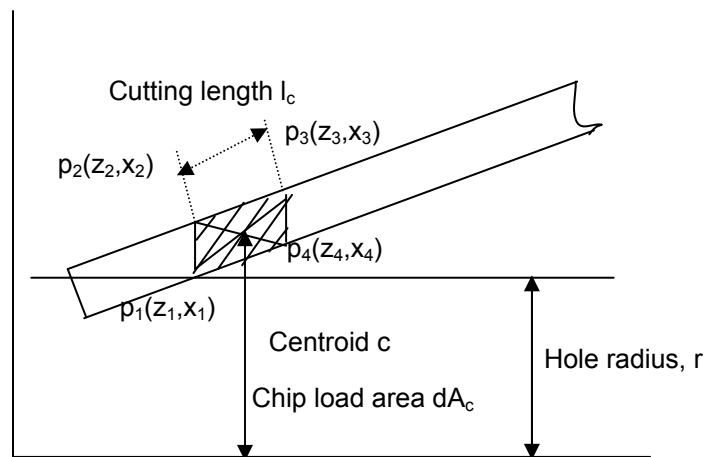
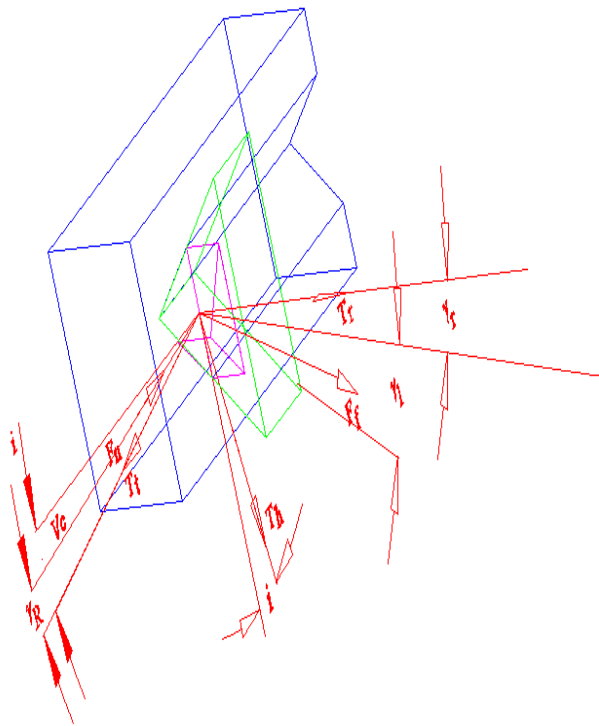


Figure 4: Chip Load Computation.

Figure 5 illustrates the various cutting forces acting on the reamer and corresponding angular positions.



Oblique cutting mechanics of reamer (wire frame model)

Figure 5: Various Cutting Forces During Reaming.

Resolving the normal and frictional force, the elementary tangential force, ' δT_t ', radial force, ' δT_r ' and thrust force, ' δT_h ', for trapezoidal section at time ' t ' is thus given as:

$$\begin{bmatrix} \delta T_t \\ \delta T_r \\ \delta T_h \end{bmatrix} = \begin{bmatrix} \cos \gamma_R \\ -\sin \gamma_R \\ -\cos \gamma_R \end{bmatrix} \delta F_n(t) + \begin{bmatrix} \sin \gamma_L + \sin \gamma_R \cos \gamma_L \\ \cos \gamma_L \cos \gamma_R \\ \sin \gamma_L - \sin \gamma_R \cos \gamma_L \end{bmatrix} \delta F_f(t) \quad (8)$$

where, ' γ_R ' is the reamer rake angle, ' γ_L ' is the chip flow angle and δT_t is equal to,

$$\delta T_t = \frac{\delta T_o(t)}{c(t)} \quad (9)$$

$\delta T_o(t)$ is the elementary torque and $c(t)$ is the distance from centroid of the interference area to the reamer axis obtained from Equation (7).

Considering the flute helix angle, ' γ ', these forces can be modified and written as:

$$\begin{bmatrix} \delta T_t \\ \delta T_r \\ \delta T_h \end{bmatrix} = \begin{bmatrix} \cos \gamma_R \sin \gamma \\ -\sin \gamma_R \\ -\cos \gamma_R \cos \gamma \end{bmatrix} \delta F_n(t) + \begin{bmatrix} \sin \gamma_L \cos \gamma + \sin \gamma_R \sin \gamma \cos \gamma_L \\ \cos \gamma_L \cos \gamma_R \\ \sin \gamma_L \sin \gamma - \sin \gamma_R \cos \gamma \cos \gamma_L \end{bmatrix} \delta F_f(t) \quad (10)$$

where the flute helix angle, ' γ ', depends upon the type of reamer. $\gamma = 90^\circ$ for a simple/straight fluted reamer, $\gamma < 90^\circ$ for spiral fluted reamers and $\gamma > 90^\circ$ for gun point reamer. Integrating the elemental force equations over the entire domain as reamer continues to enter the work piece gives the total forces.

$$\begin{aligned} T_t(t) &= \sum_{t=0}^{t_0} \delta T_t(t) \\ T_r(t) &= \sum_{t=0}^{t_0} \delta T_r(t) \\ T_h(t) &= \sum_{t=0}^{t_0} \delta T_h(t) \end{aligned} \quad (11)$$

The time increment can be obtained as:

$$\delta t = \frac{60}{N n_f} \quad (12)$$

where ' N ' is the spindle speed, ' n_f ' is the number of flutes in the reamer and ' t_0 ' is the total time taken for the reaming operation.

Chip Load Area Measurement: Tool maker's microscope is used to get the coordinates of tooth profile. Auto-CAD drawing of the reamer is drawn to get the dimensions of the tool profile and to get chip load area. For illustration, a 20 mm diameter reamer is selected and Figure 6 shows the dimensions of the reamer.

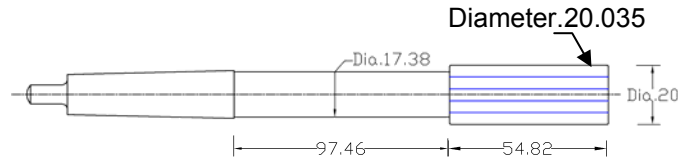


Figure 6: AutoCAD Drawing of a Reamer of 20 mm Diameter.

Static Forces in Work Piece Coordinates: The cutter geometry of one edge of the reamer tool in reaming operation shown in Figure 2 indicates the various reamer geometries such as the reamer rake angle γ_R , lead angle γ_A , and the chip flow angle γ_L . For the static cutting force transformation, co-ordinate system X, Y, Z and a, b, c are introduced. X, Y, Z co-ordinates are called global co-ordinate system, which corresponds to the work piece co-ordinate and a, b, c are the one of the cutting edge of the reamer tip co-ordinates. Even though trapezoidal cut is taking place during the reaming operation, it is assumed to be a single point oblique cutting for small interval of time.

Figure 7 shows X, Y, Z co-ordinate and a, b, c co-ordinates and transformation of T_t , T_r and T_h to individual force vector in global co-ordinates. From the global coordinates, the cutting edges of the reamer are at an angle, γ_R in radial direction which is equal to rotation in XY plane. Then it is also at an angle, γ_L in YZ plane and then γ_A in XZ plane, where γ_R , γ_L and γ_A are the reamer rake angle, chip flow angle and the lead angle respectively.

The origin of the a-b-c co-ordinate system and global co-ordinate system X-Y-Z is equal to the cutting corner of the tool tip. The force components F_T , F_R and F_A for the trapezoidal section of a reamer for rotation angle Φ can be obtained by resolving the tangential force T_t , radial force T_r , and axial force T_h acting on any tip of the reamer for a particular interval of time. For instance, consider the tangential force $F_T(t, \Phi)$, in global coordinate system which can be obtained as the summation of the tangential force components T_t , radial force T_r , and axial force T_h acting on the reamer. The T_t component can be resolved first along the lead angle γ_A and then along rake angle γ_R as $T_t \cos \gamma_A \cos \gamma_R$.

Similarly, T_r components are resolved into $T_r \cos \gamma_L \sin \gamma_R$ and axial components to $T_h \cos \gamma_L \sin \gamma_A$. Summation of the force components gives:

$$F_T(t, \phi) = T_t \cos \gamma_A \cos \gamma_R + T_h \cos \gamma_L \sin \gamma_A + T_r \cos \gamma_L \sin \gamma_R \quad (13)$$

Similarly, the cutting forces F_a and F_r can be obtained. Since cutting forces F_a and F_r are negligibly small, static torque is only computed and plotted.

RESULTS AND DISCUSSIONS

A MATLAB® program is written to simulate the static force model. The simulation results are plotted as shown in Figure 8 for different cutter sizes. As diameter and cutter length increases for particular work material, the cutting force progressively increases until to a steady state force when all the flutes are engaged in the work piece. Then suddenly cutting force falls as the reamer flutes disengage with the work piece. The plots obtained during simulation under static conditions are matching the experimental plots that were obtained for reaming process.

The general observation of torque measured during reaming is that the torque follows an almost linear path with the length of cutter till a certain point and then settles down to a kind of oscillating (sinusoidal) curve and descends down in a linear fashion which clearly indicate dynamic component of the cutting force during full length reaming.

The experiment is repeated for different work materials and Table 2 shows maximum value of torque acting on the reamer while machining aluminum and cast iron work material.

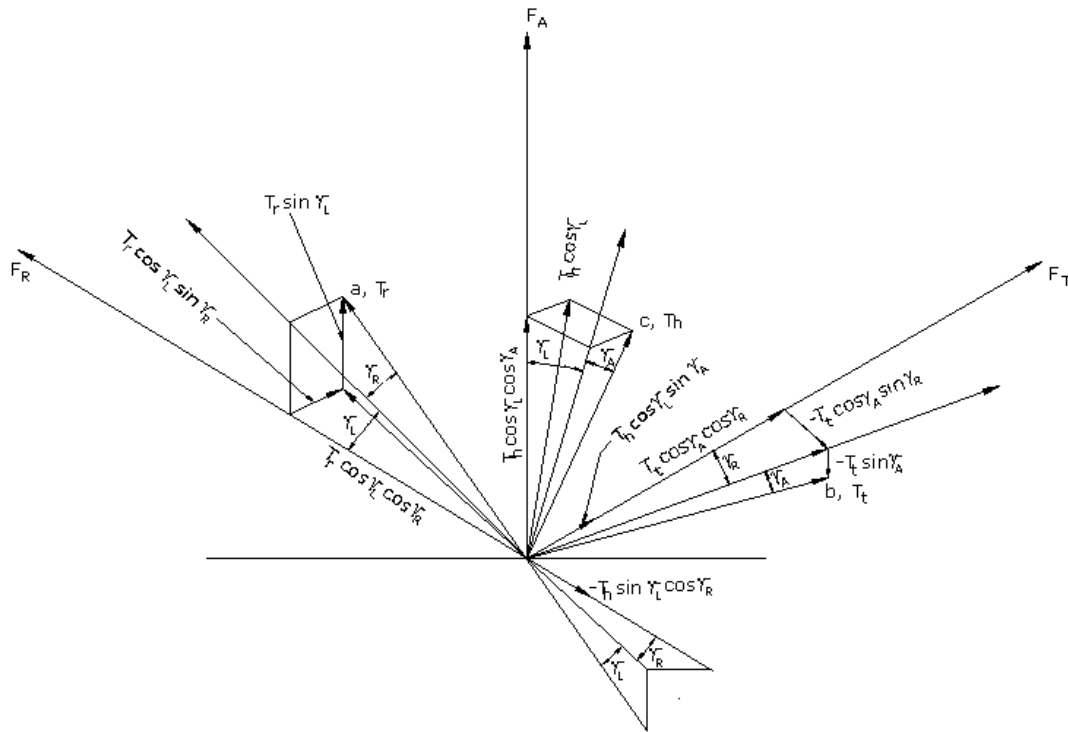


Figure 7: Force Components During Reaming Operation Shown in Work Piece Coordinate System.

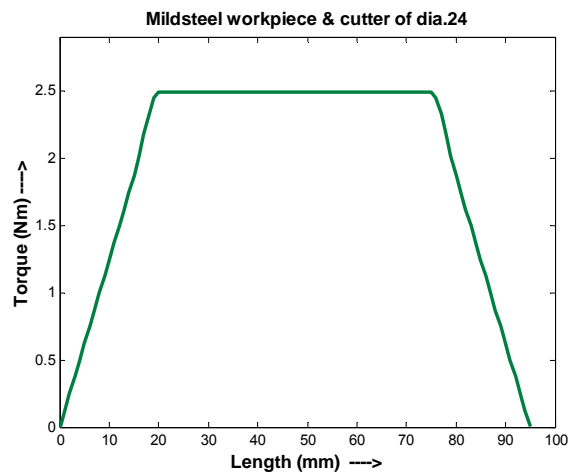
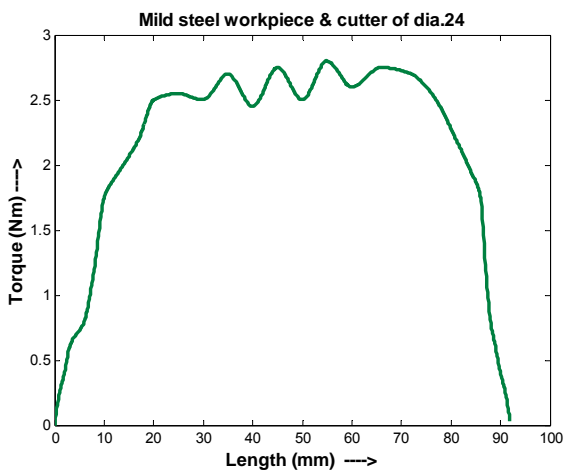
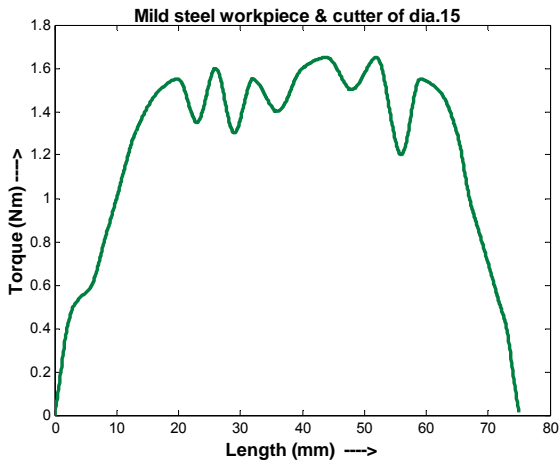
Table 2: Simulation Results of Torque for Aluminum and Cast Iron Material for Different Reamer Sizes.

Work material	Reamer diameter (mm)	Cutter length (mm)	Max. Torque (Nm)
Aluminum	30	54	0.817
	24	54.82	1.623
	20	71.52	1.978
	15	78.3	2.435
Cast iron	30	54	0.9051
	24	54.82	1.81
	20	71.52	2.172
	15	78.3	2.715

CONCLUSIONS

This paper presents the mechanistic modeling of reaming process and determination of specific cutting energy coefficients which are the determinant factors for cutting force modeling. The specific cutting energy coefficients are determined experimentally using drilling as

fundamental calibration process. The experimentally obtained results were used here for mechanistic modeling of reaming operation and results are presented graphically. The torque obtained for different sizes of the reamer experimentally are in agreement with the simulated results obtained through mechanistic modeling.



a) Experimental results

b) Simulated results for static forces

Figure 8: Experimental and Simulated Results of the Torque for Different Reamer Sizes.

NOMENCLATURE

A_c = Chip cross-section area.
 a_i, b_i, c_i = Specific cutting energy coefficients
 F_a = Axial cutting force.
 F_t = Tangential cutting force.
 F_n = Normal cutting force.
 K_t, K_n, K_a = Proportionality constants.
 t_c = chip thickness.
 v_c = cutting velocity.
 γ_a = drill rake angle

REFERENCES

1. Craig, R.R. 1981. Structural Dynamics – An Introduction to Computer Methods. Wiley: New York.
2. Belov, V.S. and Ivanov, S.M. 1974. "Factors Affecting Broaching Condition and Broach Life". *Journal of Stanki Instruments*. 45:31-33.
3. Friedman, M.Y., Kitamura, and Wu, S.M. 1974. "Rounding Mechanism of Reaming". *Annual Reports of CIRP*. 23:27-28.
4. Kim, H.S. and Ehmann, K.F., 1993. "A Cutting Force Model for Face Milling Operations". *International Journal for Machine Tools & Manufacture*. 33:651-673.
5. Lee, E.H. and B.W. Shaffer. 1951. "The Theory of Plasticity Applied to a Problem of Machining". *Journal of Applied Mechanics*. 8:405-413.
6. Merchant, M.E. 1945. "Mechanics of Metal Cutting Process-Orthogonal Cutting and a Type-2 Chip". *Journal of Applied Physics*. 16(5):267-275.
7. Merchant, M.E. 1954. "Basic Mechanics of the Metal Cutting Process". *Journal of Applied Mechanics*. 168:175-178.
8. Sakuma, K. and Kiyota, H. 1986. "Hole Accuracy with Carbide Tipped Reamers". *Bulletin of Japan Society of Precision Engineering*. 19:89-95.
9. Usui, E., A. Hiota, and M. Masuko. 1978. "Analytical Predictions of Three Dimensional Cutting Process – Part I – Basic Cutting Model: An Energy Approach". *Journal of Engineering for Industry. ASME Transaction*. 100:222-228.
10. Ya, P. Kochetkov and Yu, A. Kochetkov. 1986. "Radial Deformation of Circular Broach Teeth". *Journal of Machine Tooling*. 10:32-35.
11. Surenderan, V. 1998. "A Study of Hole Quality in Drilling". Master Thesis. University Illinois: Chicago, IL.
12. Metzler, S., Young, K.A., Bayly, P.V., and Halley, J.E. 1999. "Analysis and Simulation of Radial Chatter in Drilling and Reaming". *ASME Design Engineering Conference*: Las Vegas, NV. 12-15.
13. Bayly, P.V., Young, K.A., and Halley, J.E. 2001. "Analysis of to Oscillation and Tool Oscillation and Hole Roundness Error in a Quasi-Static Model of Reaming". *ASME Journal of Manufacturing Science and Engineering*. 123:387-396.
14. Arunachalam, S., Gunasekaran, A., and O'Sullivan, J.M. 1999. "Analyzing the Process Behaviour of Abrasive Reaming using an Experimental Approach". *International Journal of Machine Tool and Manufacturing*. 39:1311-1325.
15. Juhchin, A.Y., Venkatraman, J., and Ruxu, Du. 2002. "An Dynamic Model for Drilling and Reaming Processes". *International Journal of Machine Tool and Manufacturing*. 42:299-311.
16. Onik Bhattacharya, Shiv Kapoor. and Richard, E. Devor. 2005. "Mechanistic Model for the Reaming with Emphasis on Process Faults". *Journal of Machine Tools and Manufacture*. 1-11.

ABOUT THE AUTHORS

C. Raghavendra Kamath, BE, M.Tech., MS, is a Senior Lecturer in the Department of Mechanical and Manufacturing Engineering, MIT, Manipal, Karnataka, India. He holds a Bachelor of Engineering (B.E.) degree in Industrial Production from the Mangalore University, Karnataka in 1999. He also holds a Master of Technology (M.Tech.) in Advanced Manufacturing from National Institute of Technology, Karnataka in 2004. He is currently working towards his Doctoral degree in the area of force analysis of a manufacturing process.

Dr. K.K. Appu Kuttan, BE, ME, Ph.D. was educated at IIT Chennai. He is a professor at the National Institute of Technology, Karnataka, India. He was the Head of the Mechanical Engineering Department at the same institution. He has presented papers at National and International conferences and also published papers in National and International Journals on various aspects of Control Engineering. He has worked in various capacities in this institution at the level of Professor, Head of Mechanical Engineering Department. His area of interest includes Control

Engineering, Manufacturing Technology and thermal engineering.

SUGGESTED CITATION

Raghavendra Kamath, C. and K.K. Appu Kuttan. 2009. "Determination of Proportionality Constants from Experiments to Develop a Force Model for Reaming Process". *Pacific Journal of Science and Technology*. 10(2):57-67.

 [Pacific Journal of Science and Technology](http://www.akamaiuniversity.us/PJST.htm)